

1 **Effects of spectral smearing on performance of the spectral ripple and spectro-temporal**
2 **ripple tests**

3

4 Vijaya Kumar Narne^a

5 Department of Audiology, Gulf Medical University, Al Jerf, Ajman, 4178, UAE

6

7 Mridula Sharma^{b,c}

8 ^b *Department of Linguistics, Australian Hearing Hub, 16 University Avenue, Macquarie*
9 *University, NSW, 2109, Australia*

10

11 Bram Van Dun ^{c,d},

12 ^d *National Acoustic Laboratories, Level 5, Australian Hearing Hub, 16 University Ave,*
13 *Macquarie University, NSW 2109, Australia*

14

15 Shalini Bansal and Latika Prabhu

16 *Department of Audiology, All India Institute of Speech and Hearing, Manasagangothri,*
17 *Mysore, 570006, India*

18

19 Brian C.J. Moore

20 *Department of Experimental Psychology, University of Cambridge, Downing street,*
21 *Cambridge, CB2 3EB, UK*

22

23 a) Author to whom correspondence should be addressed. Electronic mail:

24 vijaynarne@gmail.com

25 *Keywords:* Spectral ripple; Spectral resolution; Spectral smearing; Masking

26 Second revision dated October, 2016

27

28

29

^c Also at The *HEARing CRC*, 550 Swanston Street, Department of Audiology and Speech Pathology, The University of Melbourne, Carlton VIC 3053, Australia.

30 **Abstract**

31 The main aim of this study was to use spectral smearing to evaluate the efficacy of a spectral
32 ripple test (SRt) using stationary sounds and a recent variant with gliding ripples called the
33 spectro-temporal ripple test (STRt) in measuring reduced spectral resolution. In Experiment 1
34 the highest detectable ripple density was measured using four amounts of spectral smearing
35 (unsmeared, mild, moderate and severe). The thresholds worsened with increasing smearing
36 and were similar for the SRt and the STRt across the three conditions with smearing. For
37 unsmeared stimuli, thresholds were significantly higher (better) for the STRt than for the SRt.
38 An amplitude fluctuation at the outputs of simulated (gammatone) auditory filters centered
39 above 6,400 Hz was identified as providing a potential detection cue for the STRt stimuli.
40 Experiment 2 used notched noise with energy below and above the passband of the SRt and
41 STRt stimuli to reduce confounding cues in the STRt. Thresholds were almost identical for
42 the STRt and SRt for both unsmeared and smeared stimuli, indicating that the confounding
43 cue for the STRt was eliminated by the notched noise. Thresholds obtained with notched
44 noise present could be predicted reasonably accurately using an excitation-pattern model.

45

46 I. INTRODUCTION

47 Tests of the ability to detect or discriminate spectral ripples have often been used to
48 measure the frequency selectivity of the auditory system (also called spectral resolution) and
49 to study spectral shape perception. Such tests employ a “carrier” that is either white noise or
50 multiple sinusoids covering a certain frequency range. The spectrum of the carrier is
51 modulated with a sinusoidal function on a logarithmic or a linear frequency scale (Supin *et*
52 *al.*, 1998; Won *et al.*, 2007). The result is a broadband stimulus with regular amplitude
53 fluctuations along the frequency axis (spectral modulations). The rate of spectral modulation,
54 or ripple density, is specified as the number of ripples per Hz for linearly-spaced ripples and
55 number of ripples per octave (RPO) for logarithmic spacing.

56 Spectral resolution and spectral shape perception have been studied using such stimuli
57 in several tasks. Two of the most common are (1) spectral ripple detection (Litvak *et al.*,
58 2007; Saoji *et al.*, 2009; Anderson *et al.*, 2012) and (2) spectral ripple discrimination (Supin
59 *et al.*, 1998; Won *et al.*, 2007; Aronoff and Landsberger, 2013). In the ripple detection task,
60 the ripple density is held constant in a given run and the spectral modulation depth is
61 adaptively varied to estimate the smallest spectral modulation depth (in dB) that can be
62 detected, i.e. discriminated from an unmodulated carrier. Performance is measured as a
63 function of ripple density. In the spectral ripple discrimination task, the listener is asked to
64 discriminate between a reference stimulus with a specific ripple density and a target stimulus
65 that differs from the reference in some way. There are at least two variants of this task. In
66 one, the target has the same ripple density as the reference, but the phase of the spectral
67 modulation is changed for the target (ripple phase discrimination). The smallest detectable
68 change in ripple phase as a function of modulation depth may be measured, or the smallest
69 ripple depth at which a given phase change can be detected may be measured. In the other
70 variant of the spectral ripple discrimination task, the ripple density differs for the target and

71 reference (ripple density discrimination). This second variant, estimating the smallest
72 detectable difference in ripple density, was used in the present study. However, the ripple
73 density of the reference stimulus used here was sufficiently high that the spectral ripple was
74 essentially undetectable, so the task resembled ripple detection. The highest value of the
75 ripple density of the target at which the task could be performed was measured using a fixed
76 spectral modulation depth. This test is referred to hereafter as the spectral ripple test, SRt.

77 Measures of performance on a variety of spectral ripple tests, which are usually
78 assumed to reflect frequency selectivity, have been found to be correlated with aspects of
79 hearing performance (speech and music perception) for listeners with normal hearing,
80 sensorineural hearing loss, and cochlear implants (Henry *et al.*, 2005; Litvak *et al.*, 2007;
81 Won *et al.*, 2007; Saoji *et al.*, 2009; Jones *et al.*, 2013). However, Azadpour and McKay
82 (2012) have shown that thresholds obtained using such tests may not provide an accurate
83 measure of spectral resolution for cochlear implant users, for whom even ripples with very
84 low ripple densities are hard to detect and discriminate. They reported that, apart from
85 spectral cues relating to the ripples, there were additional confounding cues, such as
86 differences in loudness, spectral centroid (the weighted mean frequency), and changing
87 energy at the spectral edges, that led to better thresholds than would be obtained if only cues
88 from the spectral ripples were used.

89 There are several ways to reduce the use of these confounding cues, including
90 randomizing the level of the stimuli as well as the starting phase of the spectral modulation.
91 However, randomizing the level can be problematic for cochlear implant users, because of
92 their very small dynamic range. Aronoff and Landsberger (2013) proposed a method for
93 reducing the use of confounding cues using a modified version of the SRt in which the phase
94 of the spectral modulation changed over time, called here the spectro-temporal ripple test
95 (STRt). As a result of the temporal changes, the overall loudness evoked in each local

96 frequency region, the energy at the spectral edges, and the spectral centroid became
97 unreliable cues for discriminating the target and reference stimuli. Aronoff and Landsberger
98 (2013) evaluated the effectiveness of the STRt in assessing spectral resolution using a ripple
99 density discrimination task. As in the present study, the ripple density of the reference
100 stimulus was sufficiently high that the task resembled spectral ripple detection. They
101 simulated reduced spectral resolution by vocoding the stimuli. They demonstrated that as the
102 number of vocoder channels decreased, simulating progressively poorer frequency
103 selectivity, the highest ripple density that could be detected also decreased, suggesting that
104 the STRt provided a measure of spectral resolution.

105 Vocoder techniques have been employed in several studies to simulate the effects of
106 reduced spectral resolution, especially for simulating the information provided by cochlear
107 implants (Shannon *et al.*, 1995; Friesen *et al.*, 2001; Litvak *et al.*, 2007; Aronoff and
108 Landsberger, 2013). However, there are limitations of this approach. For example, when a
109 noise vocoder is used, the random amplitude fluctuations in the noise carriers may affect
110 performance and the filters used to extract the channel envelopes may limit the representation
111 of cues relating to fundamental frequency (Stone *et al.*, 2008). Also, temporal fine structure
112 information may be reconstructed from envelope information (Gilbert and Lorenzi, 2006).

113 Another way to simulate reduced spectral resolution is to smear the power spectrum
114 of the signal (Baer and Moore, 1993). This method can create excitation patterns in a normal
115 ear that resemble those in an impaired ear with reduced spectral resolution. Any desired
116 degree of reduced frequency selectivity can be simulated in a quantitative manner. The
117 method gives a reasonably accurate simulation of the effect of cochlear hearing loss on
118 frequency selectivity measured using the notched-noise method (Moore *et al.*, 1992). In the
119 present study, spectral smearing was used to simulate several degrees of reduced frequency
120 selectivity. Ripple density discrimination with a high reference ripple density was compared

121 for the spectral ripple test (SRt) and the modified spectro-temporal ripple test (STRt) for each
122 degree of smearing, to assess whether the test outcomes reflected the degree of smearing and
123 to assess whether the tests gave similar results. Experiment 1 revealed a discrepancy between
124 the results of the SRt and STRt for unsmearred stimuli, but not for smeared stimuli.
125 Simulations of auditory filtering identified a potential confounding cue, not directly
126 connected with frequency selectivity, for the STRt. The cue took the form of amplitude
127 fluctuations in a frequency region outside the nominal frequency range of the stimulus.
128 Experiment 2 made use of a notched noise to mask the confounding cue and to assess its
129 influence. The results obtained in the presence of the notched noise could be predicted well
130 using an excitation-pattern model, supporting the use of the SRt and STRt tests as measures
131 of spectral resolution.

132 **II. EXPERIMENT 1**

133 **A. Method**

134 **1. *Participants***

135 There were ten normal-hearing participants (2 males and 8 females) with a mean age of
136 20 years (range: 18 – 25, standard deviation, SD = 2.4 years). Pure-tone thresholds and
137 speech identification scores were measured using a calibrated diagnostic audiometer (GSI-61,
138 Grason-Stadler, Eden Prairie, MN) with Telephonics TDH-39 headphones (Huntingdon,
139 NY). All participants had pure-tone thresholds ≤ 15 dB HL at octave frequencies between
140 0.25 and 8 kHz, as estimated using the modified Hughson and Westlake procedure (Carhart
141 and Jerger, 1959). All had identification scores for speech in quiet greater than 90% at 40 dB
142 SL (relative to the pure-tone average at 0.5, 1, 2 and 4 kHz) using word lists developed at the
143 All India Institute of Speech and Hearing (AIISH), Mysore, India. All participants had
144 normal tympanograms, with ipsilateral acoustic reflexes at normal levels in both ears,
145 indicating normal middle ear function. None of the participants had a history of neurological
146 and/or otological disorder.

147 All the testing procedures were approved by the All India Institute of Speech and

148 Hearing review board, and written informed consent was obtained from all participants.

149

150 **2. Spectral ripple stimuli**

151 The stimuli used in the SRt and the STRt were generated as described by Aronoff and
 152 Landsberger (2013). The stimuli were 750-ms long with 100-ms cosine-squared onset and
 153 offset ramps, and were sampled at 22,050 Hz. They were generated using a carrier composed
 154 of 201 equal-amplitude sinusoidal frequency components, spaced every 0.03rd octave from
 155 100 to 6,400 Hz. The amplitude of each of the sinusoids was a function of the ripple density,
 156 D (in ripples per octave, RPO), and the ripple rate (R , in ripples per s) (when temporal
 157 modulation was present, i.e., for the STRt stimuli only). The STRt stimulus as a function of
 158 time, $STRt(t)$, is defined by eq. 1 and 2:

159

$$160 \quad STRt(t) = \sum_{i=1}^{i=201} \frac{P(i)}{201} \times 10 \frac{d \left(\left| \sin(\pi R t + 0.03 i \pi D + \theta_2) \right| - 1 \right)}{20} \quad (\text{eq. 1})$$

161

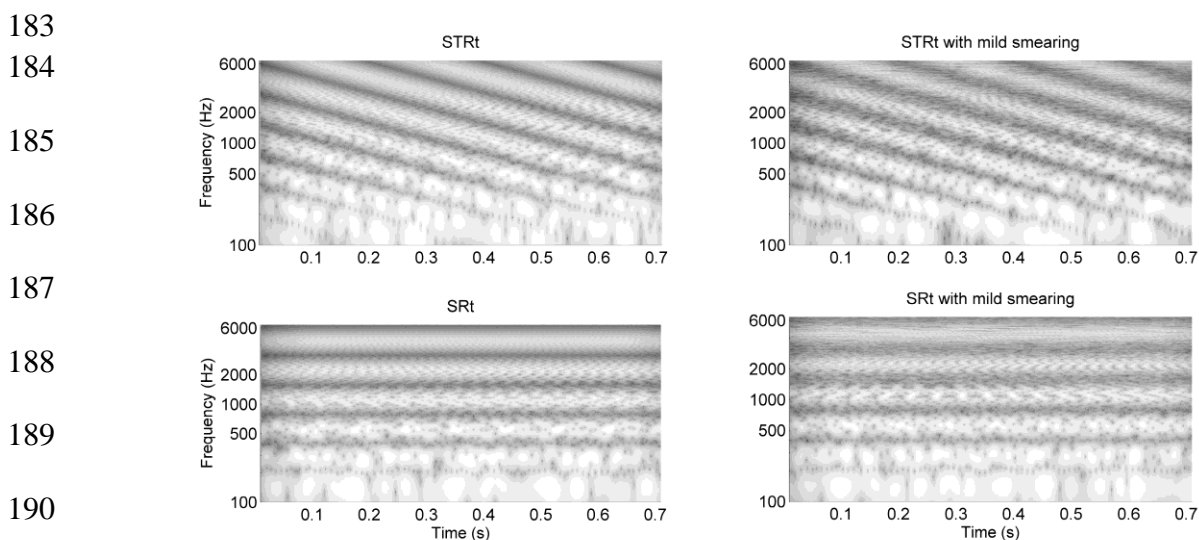
$$162 \quad \text{where} \quad P(i) = \sin(2\pi f_c(i)t + \theta_1) \quad (\text{eq. 2})$$

163 $P(i)$ is the i th carrier component with frequency $f_c(i) = 100 \times 2^{0.03(i-1)}$ ($i = 1-201$),
 164 corresponding to $f_c = 100-6400$ Hz, θ_1 is the starting phase of each sinusoidal component in
 165 the carrier, which was chosen randomly for each component over the range $0-2\pi$ radians, θ_2
 166 determines the phase of the spectral ripple at the onset of the stimulus, which was chosen
 167 randomly for each stimulus over the range $0-\pi$ radians, and d is the ripple depth in dB.¹

168 To describe eq. 1: the spectral modulator was initially a sinusoid on a logarithmic
 169 frequency scale, with spectral frequency equal to $0.5D$. This was rectified by taking the
 170 absolute value, giving a function repeating with rate D , with a value varying between 0 and 1.
 171 One was subtracted from this function to give a function varying between 0 and -1 . This was
 172 multiplied by the desired ripple depth, d , in dB. The value of the result was divided by 20 and
 173 the antilog (base 10) was taken. This sequence provided the final function that determined the
 174 amplitude of each carrier component as a function of frequency. The spectral ripples were

175 approximately, but not exactly, sinusoidal in form on a logarithmic frequency axis. For our
 176 stimuli, d was 20 dB, so the peak-to-valley ratio in the spectrum was 20 dB. For the STRt
 177 stimuli, the peaks and valleys in the spectral ripple shifted along the frequency axis such that
 178 the spectral pattern repeated every 200 ms ($R = 5$ Hz). For the SRt, R was set to zero, so the
 179 function applied to each carrier component was simply a scaling of the overall amplitude.
 180 Example spectrograms for STRt and SRt stimuli are shown in the two left panels of Fig. 1.

181 The overall level of both the unsmearred and spectrally smeared stimuli (see below)
 182 was 75 dB SPL, which was reported by participants to be comfortably loud.



191 **FIG. 1.** Spectrograms of unsmearred stimuli (left) and stimuli with mild spectral smearing
 192 (right) for the STRt (top) and the SRt (bottom). The ripple density was 1 RPO and the ripple
 193 rate was 5 Hz.

194

195 3. Simulation of reduced spectral resolution

196 The spectral smearing used in the current study was similar to that described by Baer
 197 and Moore (1993). The smearing was carried out using an overlap-add algorithm. The
 198 spectral-ripple stimulus was segmented into frames, each 256 samples (11.6 ms) long and a
 199 Hamming window was applied to each frame. The magnitude and phase of the components in
 200 each frame were extracted using a 256-point Fast Fourier Transform (FFT). The magnitude
 201 spectrum was multiplied by a smearing matrix (described in more detail below). The

202 application of an inverse FFT gave the temporal waveform of the spectrally smeared frame,
203 which was then scaled to have the same amplitude as the unsmeared signal. Finally, the time
204 waveforms were added together using 75% overlap.

205 The smearing matrix was created using the following procedure. An auditory filter
206 function was computed for each component frequency in the input spectrum. Auditory filter
207 functions were derived using the one-parameter form of the *roex(p)* filter (Patterson and
208 Nimmo-Smith, 1980). The value of p for the unsmeared stimuli varied with frequency
209 according to the equation given by Glasberg and Moore (1990). A total of 128 auditory filter
210 functions was created and stored in a 128-by-128 matrix. Widened auditory filter functions
211 were created by dividing the value of p by 3 for mild smearing, 6 for moderate smearing and
212 9 for severe smearing. The smeared matrix was derived by multiplying the inverse matrix of a
213 normal auditory filter bank [with values of p based on the equation given by Glasberg and
214 Moore (1990)] with the matrix for the widened auditory filter bank. This compensated for the
215 spectral smearing effects of the auditory filters of the normal-hearing participants. The right
216 panels of Fig. 1 show spectrograms of STRt and SRt stimuli with mild spectral smearing.

217

218 **4. Procedure**

219 All participants were seated comfortably in a quiet room. Thresholds were estimated
220 using a three-alternative forced-choice (3AFC) procedure. Two of the intervals contained a
221 reference stimulus with a ripple density of 20 RPO (for which the ripples were assumed to be
222 completely unresolved). The ripple density of the target was initially 0.5 RPO and it was
223 modified with a 2-down 1-up tracking method estimating the 70.7% correct point on the
224 psychometric function (Levitt, 1971). The step size in ripple density was initially 0.5 RPO
225 and it was decreased to 0.1 RPO after two reversals. The arithmetic mean ripple density at the
226 last six reversal points in a block of eight was taken as the threshold. All participants were

227 given two practice runs before commencing the experiment and a single threshold estimate
228 was obtained for each condition and each participant. The ripple density at threshold was
229 never higher than 10 and the ripple density of the target never became close to that of the
230 reference during an adaptive track.

231 MATLAB 7.10.0 (Mathworks; Natick, MA, USA) software installed on a personal
232 computer (PC) was used to control stimulus presentation. The stimuli were presented via a
233 PC fitted with a 32 bit Realtek high definition sound card and routed through an audiometer
234 (Madsen OB-922) to the headphones (TDH-39 with MX 41/AR cushions). The order of
235 testing of the stimulus conditions was randomized across participants.

236

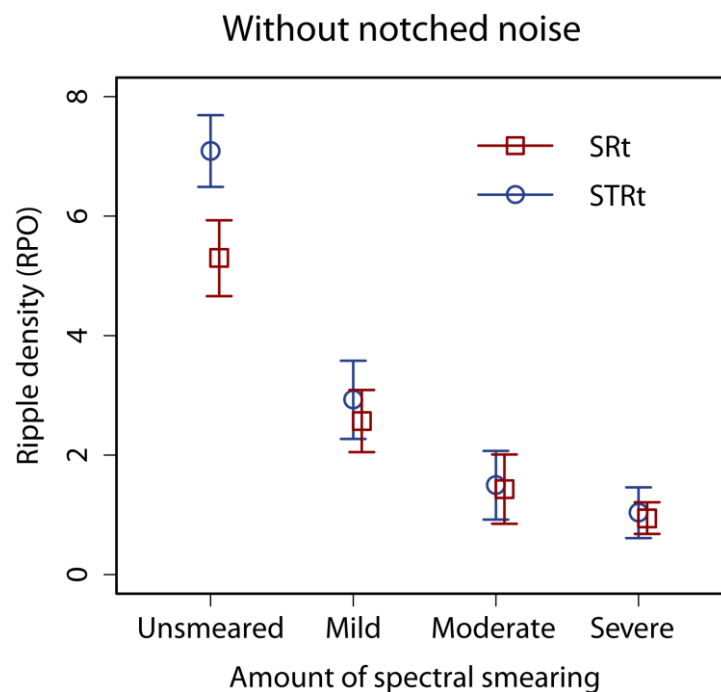
237 **5. Statistical analysis**

238 Modern statistical techniques were employed to minimize the potential effects of any
239 outliers or non-normality in the data [for more details, see (Wilcox, 2012a)]. These statistical
240 techniques employ 20% trimmed means, which are a cross between a mean and a median.
241 Since there were 10 participants, 20% trimming meant that the thresholds for the worst-
242 performing and best-performing participant in each condition were discarded. Trimmed
243 means were used to estimate the means shown in the figures, for analyses of variance
244 (ANOVAs), and for post hoc tests. Bootstrap techniques were also employed, which allow
245 tests to be conducted using distributions based on the original data set rather than on assumed
246 normal distributions that may not accurately reflect the data (Wilcox, 2012a). All analysis
247 was performed using the WRS package in R 3.2.3 (Wilcox, 2012b). Thresholds across the
248 four conditions of spectral smearing (i.e., unsmearing, mild, moderate and severe smearing)
249 using the two tests (SRt and STRt) were compared using a within-subjects ANOVA (Wilcox,
250 2012b).

251

252 B. Results

253 The results are shown in Fig. 2. The highest ripple density of the target at which it
 254 could just be discriminated from the reference is plotted for each test and each smearing
 255 condition. There was a significant main effect of smearing condition ($F_t = 18.03$, $p < 0.0001$),
 256 increasing spectral smearing resulting in decreasing (poorer) ripple thresholds. There was a
 257 significant main effect of test type ($F_t = 156.78$, $p < 0.0001$), the STRt giving higher ripple
 258 thresholds than the SRt. There was a significant interaction ($F_t = 5.96$, $p < 0.001$) between
 259 smearing condition and test type. To investigate the interaction, multiple comparisons with
 260 Rom's method for controlling familywise error (Rom, 1990) were performed. All of the
 261 smearing conditions except moderate and severe were significantly different from one
 262 another ($p < 0.001$) for both the STRt and the SRt. Pairwise comparisons were performed
 263 using Yuen's method. Thresholds were significantly higher (better) for the STRt than for the
 264 SRt only for the condition with no smearing ($p < 0.001$).



265

266 **FIG. 2.** Trimmed means with error bars (95% confidence intervals estimated using 20%
 267 trimmed mean and bootstrapping method) for each spectral smearing condition, for the SRt
 268 (circles) and the STRt (squares) (color online). For visual clarity, data points are plotted
 269 slightly offset from their correct positions along the x-axis.

270 C. Discussion

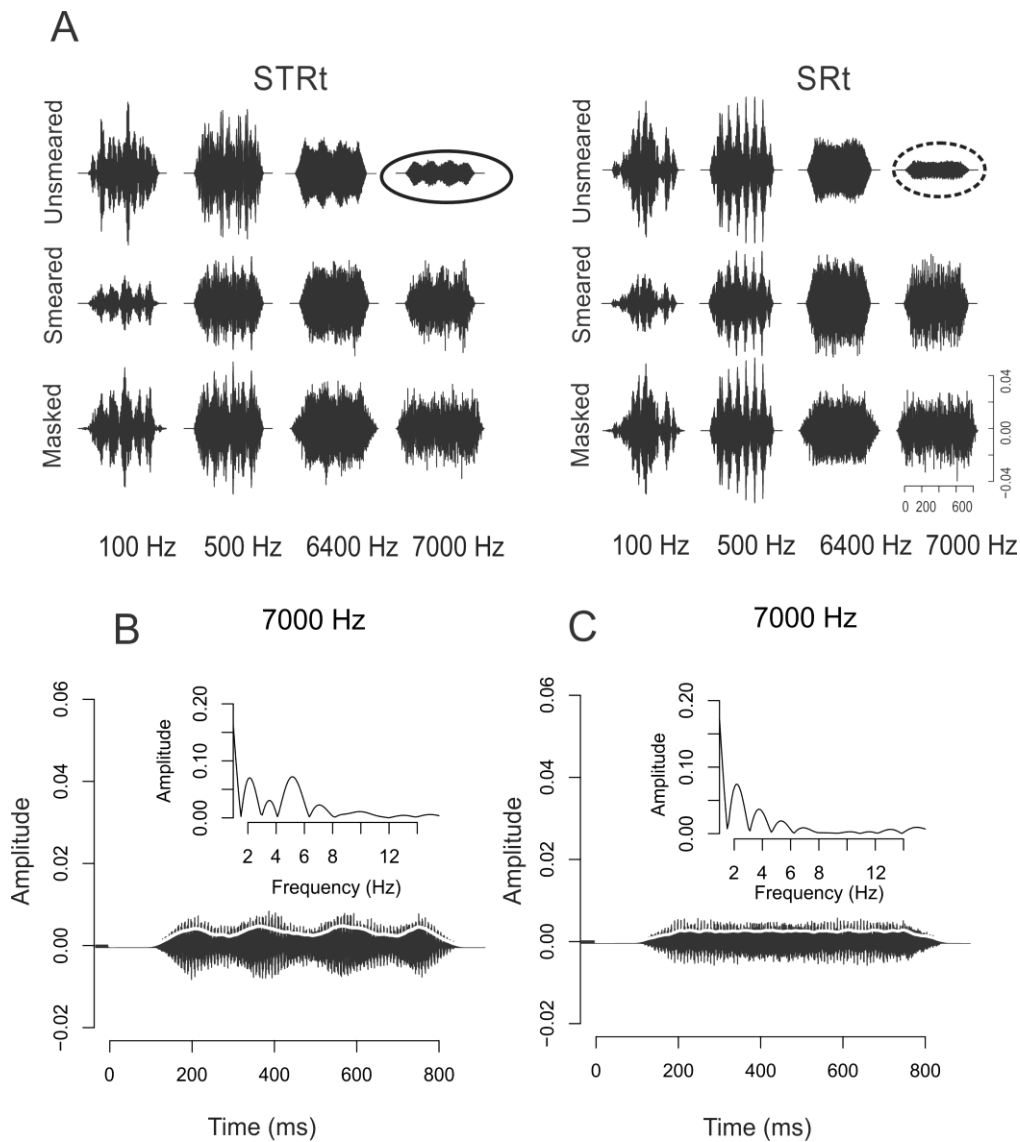
271 Increasing the amount of spectral smearing, simulating progressive broadening of the
272 auditory filters, resulted in a significant decrease of ripple thresholds (indicating poorer
273 spectral resolution) for both the SRt and STRt. This clearly shows that both the SRt and the
274 STRt are sensitive to simulated changes in frequency selectivity.

275 The mean ripple threshold for the STRt stimuli in the condition without smearing was
276 approximately 7.1 RPO, which is slightly less than the mean threshold of 8.2 RPO reported
277 by Aronoff and Landsberger (2013). The difference in mean threshold across studies may be
278 due to the use of different tracking rules. While both studies used a 3AFC procedure, Aronoff
279 and Landsberger (2013) estimated the threshold corresponding to 50% correct using a 1-up 1-
280 down procedure, which tracks $d' = 0.56$, whereas in the present study threshold was estimated
281 at the 70.7% correct point using a 2-down 1-up procedure, which tracks $d' = 1.28$. The mean
282 threshold for the SRt stimuli in the condition without smearing was 5.7 RPO which is similar
283 to the mean threshold of 5.5 RPO found by Henry *et al.* (2005) and Peter *et al.* (2014). The
284 higher thresholds for the STRt stimuli than for the SRt stimuli may have occurred because
285 additional cues were available for the STRt stimuli in the condition without smearing.

286 Without smearing, both the STRt and SRt stimuli had sharp spectral edges at 100 and
287 6,400 Hz. The spectral smearing would have removed these sharp spectral edges. Hence, it
288 seems likely that whatever extra cue was available for the STRt stimuli without smearing was
289 connected with the sharp spectral edges. It was hypothesized that STRt stimuli with no
290 smearing produced amplitude fluctuations at the outputs of auditory filters centered above
291 6,400 Hz, and that these fluctuations provided a detection cue. To assess this hypothesis,
292 STRt and SRt stimuli with a ripple density of 7 RPO (i.e. above the threshold for the SRt test
293 with unsmearred stimuli) were passed through an array of 4th order gammatone filters, which
294 provide a model of the auditory filters (Patterson *et al.*, 1995). The bandwidths of the filters

295 were as specified by Glasberg and Moore (1990). The waveforms at the outputs of some of
296 the simulated auditory filters are shown in part A of Fig. 3. These filters were selected
297 because they revealed possible cues for the unsmeared STRt stimuli that were not present for
298 the SRt stimuli. The unsmeared STRt stimuli (top) led to distinct regular amplitude
299 fluctuations corresponding to the R of 5 Hz at the outputs of simulated auditory filters centred
300 at 6,400 and 7000 Hz (see the waveform highlighted by ovals), but not for lower center
301 frequencies. These fluctuations are more clearly visible in panel B, which shows the
302 waveform at the output of the simulated auditory filter centered at 7000 Hz, with the
303 envelope superimposed (white trace). The envelope shown is the Hilbert envelope after
304 lowpass filtering using a finite-impulse-response filter with a cutoff frequency of 100 Hz. The
305 modulation depth of the envelope was about 25%. The inset in panel B shows the spectrum of
306 the envelope, which has a clear peak at 5 Hz, corresponding to the R . There was no peak at 5
307 Hz in the spectrum of the envelope of the reference stimulus (not shown), so the 5-Hz
308 envelope fluctuation provided a potential detection cue for the STRt stimuli. As shown in
309 panel C, there was no peak in the spectrum of the envelope at 5 Hz for the SRt stimulus.
310 When smearing was introduced, the amplitude fluctuation at 5 Hz was absent for both the
311 STRt and the SRt stimuli.

312



313

314 **FIG. 3.** Part A shows waveforms at the outputs of simulated auditory (gammatone) filters
 315 with selected center frequencies for STRt stimuli (left) and SRt stimuli (right) with a ripple
 316 density of 7 RPO for three conditions: unsmear (“Unsmear”), severely smeared
 317 (“Smear”), and unsmear with notched-noise added (“Mask”). The filter center
 318 frequency in Hertz is indicated at the bottom. The amplitude scale is arbitrary, but the
 319 scaling was the same for all stimuli. The ovals highlights waveforms at the outputs of filters
 320 centered at 7000 Hz, showing 5-Hz amplitude modulation for the unsmear STRt stimuli but
 321 not the unsmear SRt stimuli. This is illustrated in more detail in panels B and C, which
 322 show the waveform and envelope (white trace) at the output of the auditory filter centered at
 323 7000 Hz for the unsmear STRt and SRt stimuli, respectively. The insets in panels B and C
 324 show the spectra of the envelopes, which have a peak at 5 Hz for the STRt but not for the SRt
 325 stimuli.

326

327

328

329 For the SRt unsmearred stimuli (and to a lesser extent for the smeared stimuli), regular
330 envelope fluctuations are apparent at the output of the gammatone filter centered at 500 Hz.
331 These fluctuations are a consequence of beats between adjacent sinusoidal components in the
332 carrier, whose spacing was approximately 10.5 Hz at the center frequency of 500 Hz. Such
333 beats also occurred at the outputs of other gammatone filters (with higher rates for higher
334 center frequencies), but they are not easily visible in the waveforms. The beats were present
335 for both the test and reference stimuli and so presumably did not provide a cue for detecting
336 the spectral ripple.

337

338 **III. EXPERIMENT 2**

339 To assess whether cues at the outputs of auditory filters centered above 6,400 Hz led
340 to better performance for the unsmearred STRt stimuli than for the unsmearred SRt stimuli, a
341 second experiment was performed in which notched noise was added to all stimuli, to make
342 such cues unusable.

343

344 **A. Method**

345 ***1. Participants***

346 There were ten normal-hearing participants (4 males and 6 females) with a mean age
347 of 25 years (range: 20 – 35 years, SD = 5.3). Their characteristics were the same as for
348 Experiment 1.

349

350 ***2. Stimulus, procedure and statistical analysis***

351 The stimuli were the same as used in Experiment 1 except that sharply filtered
352 (digitally generated) notched noise was added to all stimuli. The notched noise onset
353 preceded the onset of each stimulus by 100 ms and the notched noise continued for 100 ms
354 after the end of the stimulus. The noise was ramped on and off using a cosine-squared
355 function with ramp duration of 100 ms. The lower and upper edge frequencies of the notch
356 were 100 and 6,400 Hz, respectively, coinciding with the edge frequencies of the SRt and
357 STRt stimuli. The root-mean-square level of the notched noise was 10 dB below that of the

358 SRt and STRt stimuli. This relative level was chosen based on the outputs of the simulated
359 auditory filters, so that the amplitude fluctuations above 6,400 Hz would be completely
360 masked while the notched noise had minimal effects on the outputs of auditory filters
361 centered between 100 and 6,000 Hz. The influence of the notched noise is illustrated in Fig. 3
362 by the rows labelled “Masked”. Procedures were identical to those for Experiment 1.

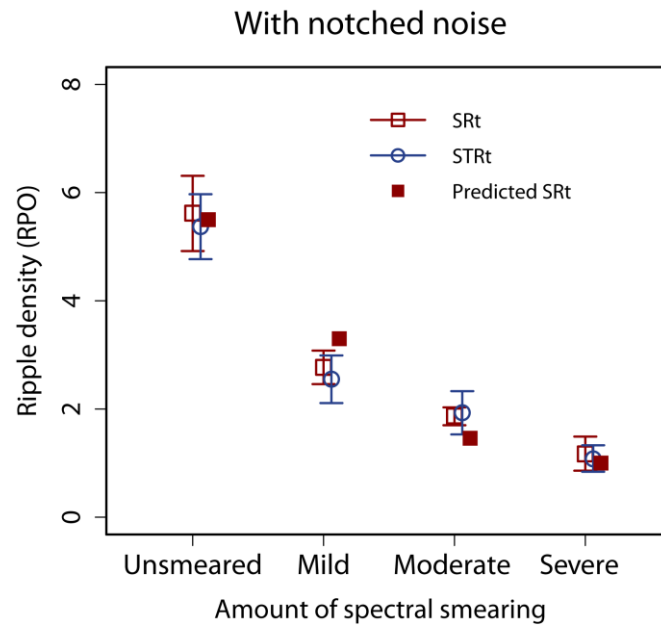
363

364 **B. Results**

365 The results of experiment 2 are shown in Fig. 4 by the open symbols. To assess
366 whether the notched noise had any significant effect on ripple threshold across the four
367 smearing conditions for the SRt and the STRt tests, the data for experiments 1 and 2 were
368 compared using a mixed-model ANOVA. Amount of smearing and test condition were
369 within-subject factors, and presence/absence of notched noise was a between-subjects factor.
370 A significant main effect of amount of smearing was found ($F_t = 96.2, p < 0.0001$), thresholds
371 decreasing with increasing spectral smearing, as expected. There was a main effect of test
372 type ($F_t = 9.8, p = 0.001$), thresholds being higher for the STRt than for the SRt. There was
373 no significant main effect of the presence/absence of notched noise ($F_t = 0.14, p = 0.72$).
374 However, there was a significant interaction of test type and presence/absence of noise ($F_t =$
375 $6.1, p=0.013$). All other two-way and three-way interactions were not significant ($p > 0.05$).

376

377



378

379 **FIG. 4.** As Fig. 2 but for stimuli presented together with notched noise. Thresholds predicted
 380 using the excitation-pattern model are shown by filled symbols.

381

382 To assess the effect of the notched noise on ripple thresholds, planned comparisons
 383 were performed using Yuen’s test. The addition of notched noise led to a significantly
 384 decreased mean threshold for the STRt unsmearred stimuli ($T_y = 4.80$, $p = 0.0013$); the
 385 decrease was 1.5 RPO. The effect of the notched noise was not significant for any other
 386 amount of smearing ($p > 0.05$).

387 When the notched noise was present, there was no significant difference between the
 388 thresholds for the STRt and SRt stimuli in the unsmearred condition ($T_y = -0.12$, $p = 0.9$).
 389 This confirms that the cues that led to better performance for the STRt than for the SRt
 390 stimuli in experiment 1 were removed by the notched noise used in experiment 2.

391

392 **C. Discussion**

393 The results support the hypothesis that amplitude fluctuations at the outputs of
 394 auditory filters centered above 6,400 Hz provided a cue that led to higher (better) thresholds
 395 for the STRt than for the SRt stimuli in the unsmearred condition. The addition of notched

396 noise eliminated these cues. The addition of notched noise did not significantly affect
397 thresholds for any of the conditions involving spectral smearing, probably because the
398 spectral smearing eliminated the sharp spectral edges of the unsmearred stimuli, so that the
399 high-frequency cues were not available. The similarity of results for the SRt and STRt when
400 notched noise was present suggests that similar cues were used to perform the two tests, for
401 example ripples in the excitation patterns evoked by the stimuli; see below for further
402 analyses based on excitation patterns. Although the STRt could in principle be performed by
403 monitoring fluctuations in the output of a single auditory filter, the similarity of the results for
404 the SRt and STRt when notched noise was present suggests that the test was not performed in
405 this way.

406 It should be noted that although spectral smearing was applied to the stimuli for the
407 spectral-ripple tests, no such smearing was applied to the notched noise. Furthermore, all the
408 participants had normal hearing. When spectral ripple tests are used for listeners with reduced
409 spectral resolution, the addition of notched noise might have a greater deleterious effect than
410 found here. Thus, while the addition of notched noise has the desirable effect of eliminating
411 confounding cues, giving a more valid measure of spectral resolution, it potentially has the
412 undesirable effect of impairing spectral ripple discrimination by producing some masking of
413 the components of the test and reference stimuli.

414 An alternative approach to reducing cues associated with sharp spectral edges is to
415 avoid spectral edges by applying a spectral window to the test and reference stimuli. For
416 example, Supin and co-workers (Supin *et al.*, 1994, 1998) have applied a Gaussian-shaped
417 spectral envelope to rippled-spectrum stimuli. A potential disadvantage of this approach is
418 that spectral ripples within the stimulus passband may produce “combination ripples” (like
419 combination tones, especially $2f_1-f_2$) outside the passband, and these combination ripples
420 may be more resolvable than the ripples within the passband. For example, if peaks in the

421 rippled spectrum occur at 2 and 2.3 kHz (corresponding to a ripple density of 5 RPO),
422 combination ripples would occur at 1.4 and 1.7 kHz (corresponding to a more resolvable
423 ripple density of 3.6 RPO). These combination ripples can be masked with a lowpass noise or
424 notched noise, but again with the potential disadvantage that the added noise has a masking
425 effect on the ripples within the passband.

426 The STRt was introduced as a modification of the SRt to prevent participants using
427 extraneous cues that might be available with the SRt stimuli. Such cues include differences in
428 overall loudness in specific frequency regions, differences in spectral centroid, and changing
429 energy at the spectral edges of the stimuli. However, for our results, thresholds were never
430 poorer for the STRt than for the SRt. This suggests either that the extraneous cues were not
431 used in the SRt or that the temporal modulation in the STRt stimuli did not prevent the use of
432 such cues. However, the extraneous cues in the SRt might be used by cochlear implantees
433 (Azadpour and McKay, 2012), for whom the ripple density at threshold is much lower than
434 for normal-hearing listeners.

435 **IV. PREDICTIONS USING AN EXCITATION-PATTERN MODEL**

436 In this section, we assess the accuracy with which the results of experiment 2 can be
437 explained using an excitation-pattern model. The excitation pattern of a sound is defined as
438 the output of each auditory filter as a function of the center frequency of the filter (Moore and
439 Glasberg, 1983). We tested the hypothesis that the threshold corresponds to a fixed peak-to-
440 valley ratio, PVR (in dB), of the ripples in the excitation pattern, as proposed by previous
441 researchers for similar stimuli (Green, 1988; Nechaev and Supin, 2013). Good accuracy of
442 the predictions would support the use of the SRt and STRt as measures of spectral resolution.
443 For a given ripple density, the spectral ripples were the same for the SRt and STRt stimuli,
444 except that the ripples were static for the former and dynamically changing for the latter. The
445 PVR of the ripples in the excitation pattern should therefore be the same for the two stimulus
446 types, and so thresholds predicted on the basis of our hypothesis should be the same for the

447 two cases. Therefore, in what follows, excitation patterns were calculated only for the SRt
448 stimuli.

449 Excitation patterns were calculated for 500 ms segments at the temporal center of the
450 stimuli. The segments were hamming windowed prior to calculation of the Welch power
451 spectra. The excitation patterns were calculated from the spectra using the Loudness toolbox
452 implemented in MATLAB (Genesis, 2010), which is based on the procedure described by
453 (Moore *et al.*, 1997). The transfer function of the TDH-39 headphones was taken into account
454 in the calculations. For each stimulus, the excitation pattern was calculated for five different
455 samples, and the resulting patterns were averaged. This was done to reduce small random
456 fluctuations caused by the random phases of the frequency components in the carrier.

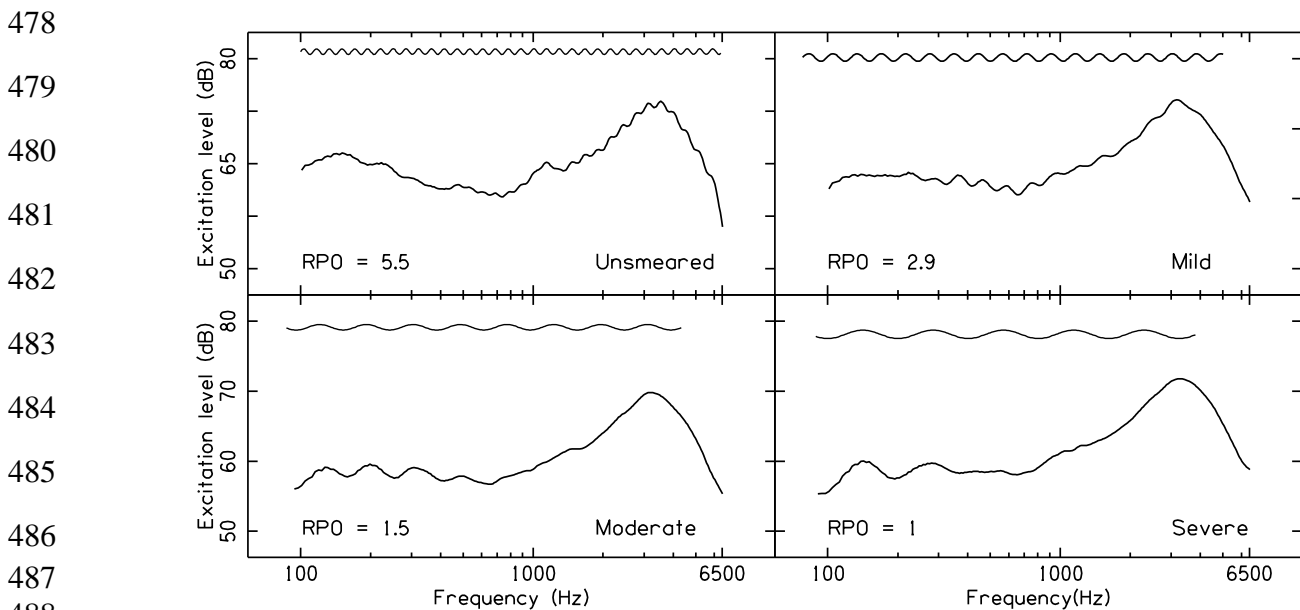
457 The first step in the modelling was to estimate the value of the PVR for each
458 condition. This was done as follows:

- 459 1) For each amount of smearing, an excitation pattern was calculated for a SRt stimulus with
460 ripple density corresponding to the mean measured threshold for that amount of smearing.
461 Examples of the excitation patterns are shown in Figure 5.
- 462 2) For each calculated excitation pattern, the region in the pattern where the ripples were
463 largest was determined and the PVR of the ripples in that region was estimated.
- 464 3) The estimates of the PVR determined in (2) were similar across unsmeared and smeared
465 conditions, which is consistent with our hypothesis. An average PVR was estimated across
466 conditions. This gave the estimated threshold criterion, i.e. the PVR in the excitation pattern
467 required for threshold. The resulting value was 1.36 dB. This value is comparable to the
468 values used in other comparable simulations (Green, 1988; Nechaev and Supin, 2013).

469 To further test the hypothesis, we predicted ripple thresholds as a function of amount
470 of smearing. If the hypothesis is accurate, the predicted thresholds should be close to the
471 obtained thresholds. To generate these predictions, the following steps were performed:

- 472 1) For each amount of smearing, excitation patterns were calculated for stimuli with ripple
473 density varying from 0.5 to 7 RPO in 0.5-RPO steps.
- 474 2) The maximum ripple depth in each excitation pattern determined in (1) was estimated.
- 475 3) The ripple density leading to a peak-to-valley ratio in the excitation pattern of 1.36 dB was

476 estimated by interpolation for each amount of smearing. The ripple density estimated in this
 477 way is the predicted ripple threshold for that amount of smearing.



489 **FIG. 5.** Examples of excitation patterns for stimuli with different degrees of spectral
 490 smearing. For each degree of smearing, the ripple density corresponded to the mean
 491 measured threshold. In each panel, a sine wave with frequency equal to the ripple density of
 492 the stimulus is plotted above the excitation pattern for visual guidance. The phase of the sine
 493 wave relative to the ripple in the excitation pattern is arbitrary.

494

495 The thresholds predicted using the model are plotted in Fig. 4 as filled symbols. The
 496 predicted thresholds are similar to the experimentally obtained data for experiment 2. This
 497 supports the idea that both the STRt and the SRt assess the spectral resolution of the auditory
 498 system. However, this does not rule out the possibility that temporal cues are used in the
 499 performance of both tasks. The use of temporal cues has been proposed to underlie the
 500 detection and discrimination of stimuli with spectral ripples that are uniformly spaced on a
 501 linear frequency scale, such as iterated rippled noise (Yost *et al.* 1996). It is not known
 502 whether such cues also play a role in the detection of spectral ripples that are uniformly
 503 spaced on a logarithmic scale, as used here and in other studies (Supin *et al.*, 1994, 1998).

504 In Fig. 5, the ripples in the excitation pattern are most prominent for the unsmeared
 505 stimuli over the frequency range from about 800 to 6000 Hz. This occurs because the relative
 506 bandwidths of the auditory filters (ERB_N /center frequency) are smallest at medium and high
 507 frequencies. However, for the stimuli with mild, moderate and severe amounts of spectral

508 smearing, the ripples are most pronounced over the ranges 300 to 2000 Hz, 100 to 500 Hz,
509 and 100 to 300 Hz, respectively. These changes with degree of smearing probably reflect side
510 effects of the way that the spectral-smearing algorithm works. The algorithm preserves the
511 phases of the components in the spectrum. As a result, when the output signal is constructed
512 from overlapping frames, the spectral structure of the original signal is partly reconstructed
513 (Baer and Moore, 1993). The effects of this reconstruction are most apparent at low and
514 medium frequencies.

515 The excitation patterns in Fig. 5 illustrate a drawback with the SRt and STRt. In
516 principle, the tests can be performed if the ripples in the excitation pattern are detectable in
517 any small frequency region. The stimuli are broadband, but there is no straightforward way of
518 assessing what frequency region is used to perform the tasks or how wide that frequency
519 region is. Furthermore, the frequency region can shift depending on the spectral resolution of
520 the participant and the way that spectral resolution varies with frequency. Researchers who
521 plan to use the SRt and STRt should bear in mind that the task does not provide a global
522 measure of frequency resolution; rather it provides a measure of the best frequency resolution
523 available to a participant for any center frequency within the passband of the stimuli.
524

525 **V. SUMMARY AND CONCLUSIONS**

526 1. As expected, simulation of one effect of cochlear hearing loss by spectral smearing
527 significantly decreased (impaired) thresholds for both the SRt and the STRt, confirming that
528 the tests are sensitive to the effects of reduced spectral resolution. Measured thresholds were
529 similar for the two tests, except when no smearing was applied. In the latter case, thresholds
530 were higher (better) for the STRt than for the SRt.

531 2. The higher threshold for the STRt in the unsmear condition could be explained by
532 amplitude modulation cues at the outputs of auditory filters centered at the upper edge of or
533 above the frequency range of the STRt stimulus. Adding notched noise eliminated the
534 confounding cues in the unsmear STRt stimuli and led to similar thresholds for the SRt and

535 the STRt. This suggests that, for normal-hearing participants, similar cues are used to perform
536 the SRt and the STRt when confounding cues are eliminated.

537 3. An excitation-pattern model based on the hypothesis that the threshold in both the SRt
538 and the STRt corresponds to a fixed peak-to-valley ratio in the excitation pattern evoked by
539 the stimuli gave reasonably accurate predictions of the way that thresholds changed across
540 smearing conditions for the data obtained in the presence of notched noise. This is consistent
541 with the idea that both tasks were performed primarily using spectral cues. However, the
542 possibility that temporal cues were used cannot be ruled out.

543 The experimental data and the predictions of the model indicate that both the SRt and
544 the STRt can be employed to estimate spectral resolution. However, when STRt stimuli are
545 used to test participants with normal hearing, notched noise should be added to eliminate cues
546 arising in frequency regions outside the passband of the stimuli. The addition of notched
547 noise may also be advisable when testing participants with hearing loss, although in this case
548 the notched noise may have an effect on the detection of ripples within the passband of the
549 stimuli. The optimal level of the notched noise remains to be determined. Researchers who
550 plan to use the SRt and STRt should bear in mind that the task provides a measure of the best
551 frequency resolution available to a participant for any center frequency within the passband
552 of the stimuli.

553

554 **Acknowledgements**

555 The authors acknowledge with gratitude Prof. S. R. Savithri, Director, All India
556 Institute of Speech and Hearing, Mysore for permitting this study to be conducted at the
557 institute. We extend our sincere thanks to Prof. Rand Wilcox for providing guidance on
558 statistical analysis of the data. We also extend our thanks to Dr. Justin Aronoff and Dr. Tom
559 Bear for their technical support and stimulus generation. The authors would also like to

560 acknowledge the participants for their co-operation and to thank Virginia Richards and two
561 reviewers for helpful comments on an earlier version of this paper.

562

563 **Footnotes**

564 1. Equation 1 in Aronoff and Landsberger (2013) does not include the step of taking the
565 antilog. However, the Matlab code provided by Justin Aronoff indicates that the antilog was
566 taken. Also, their equation 1 indicates that scaling by the ripple depth d (their term “ D ”) was
567 applied after 1 had been added to the absolute value of the sinusoid, whereas the Matlab code
568 indicates that 1 was subtracted from the absolute value of the sinusoid.

569

570 **References**

- 571 Anderson, E. S., Oxenham, A. J., Nelson, P. B., and Nelson, D. A. (2012). “Assessing the
572 role of spectral and intensity cues in spectral ripple detection and discrimination in
573 cochlear-implant users,” *J. Acoust. Soc. Am.*, **132**, 3925–3934.
- 574 Aronoff, J. M., and Landsberger, D. M. (2013). “The development of a modified spectral
575 ripple test,” *J. Acoust. Soc. Am.*, **134**, 217–222. doi:10.1121/1.4813802
- 576 Azadpour, M., and McKay, C. M. (2012). “A psychophysical method for measuring spatial
577 resolution in cochlear implants,” *J. Assoc. Res. Otolaryngol.*, **13**, 145–57.
578 doi:10.1007/s10162-011-0294-z
- 579 Baer, T., and Moore, B. C. J. (1993). “Effects of spectral smearing on the intelligibility of
580 sentences in noise,” *J. Acoust. Soc. Am.*, **94**, 1229. doi:10.1121/1.408176
- 581 Carhart, R., and Jerger, J. F. (1959). “Preferred method for clinical determination of pure-
582 tone thresholds,” *J. Speech Hear. Disord.*, **24**, 330–345.
- 583 Friesen, L., Shannon, R., Baskent, D., and Wang, X. (2001). “Speech recognition in noise as
584 a function of the number of spectral channels: comparison of acoustic hearing and
585 cochlear implants,” *J. Acoust. Soc. Am.*, **110**, 1150–1163.
- 586 Genesis, S. . (2010). *Loundness Toolbox*, <http://www.genesis.fr>, Available:
587 <http://www.genesis.fr>. Retrieved from <http://www.genesis.fr>
- 588 Gilbert, G., and Lorenzi, C. (2006). “The ability of listeners to use recovered envelope cues
589 from speech fine structure,” *J. Acoust. Soc. Am.*, **119**, 2438–2444.
590 doi:10.1121/1.2173522

- 591 Glasberg, B. R., and Moore, B. C. . (1990). “Derivation of auditory filter shapes from
592 notched-noise data,” *Hear. Res.*, **47**, 103–138. doi:10.1016/0378-5955(90)90170-T
- 593 Green, D. . (1988). *Profile Analysis*, Oxford University Press, Oxford, 1-144 pages.
- 594 Henry, B. A., Turner, C. W., and Behrens, A. (2005). “Spectral peak resolution and speech
595 recognition in quiet: normal hearing, hearing impaired, and cochlear implant listeners,”
596 *J. Acoust. Soc. Am.*, **118**, 1111–1121. doi:10.1121/1.1944567
- 597 Jones, G. L., Won, J. H., Drennan, W. R., and Rubinstein, J. T. (2013). “Relationship
598 between channel interaction and spectral-ripple discrimination in cochlear implant
599 users,” *J. Acoust. Soc. Am.*, **133**, 425–33. doi:10.1121/1.4768881
- 600 Levitt, H. (1971). “Transformed up-down methods in psychoacoustics,” *J. Acoust. Soc. Am.*,
601 **49**, 467–477.
- 602 Litvak, L. M., Spahr, A. J., Saoji, A. A., and Fridman, G. Y. (2007). “Relationship between
603 perception of spectral ripple and speech recognition in cochlear implant and vocoder
604 listeners,” *J. Acoust. Soc. Am.*, **122**, 982–91. doi:10.1121/1.2749413
- 605 Moore, B. C. J., and Glasberg, B. R. (1983). “Suggested formulae for calculating auditory-
606 filter bandwidths and excitation patterns,” *J. Acoust. Soc. Am.*, **74**, 750–753.
- 607 Moore, B. C. J., Glasberg, B. R., and Baer, T. (1997). “A model for the prediction of
608 thresholds, loudness, and partial loudness,” *J. Audio Eng. Soc.*, **45**, 224–240. Retrieved
609 from <http://www.aes.org/e-lib/browse.cfm?elib=10272>
- 610 Moore, B. C. J., Glasberg, B. R., and Simpson, A. (1992). “Evaluation of a method of
611 simulating reduced frequency selectivity,” *J. Acoust. Soc. Am.*, **91**, 3402–3423.
612 doi:10.1121/1.402830
- 613 Nechaev, D. I., and Supin, A. Y. (2013). “Hearing sensitivity to shifts of rippled-spectrum
614 patterns,” *J. Acoust. Soc. Am.*, **134**, 2913–22. doi:10.1121/1.4820789
- 615 Patterson, R. D., Allerhand, M., and Giguère (1995). “Time-domain modeling of peripheral
616 auditory processing: a modular architecture and a software platform,” *J. Acoust. Soc.*
617 *Am.*, **98**, 1890–1984.
- 618 Patterson, R. D., and Nimmo-Smith, I. (1980). “Off-frequency listening and auditory-filter
619 asymmetry,” *J. Acoust. Soc. Am.*, **67**, 229–245. doi:10.1121/1.383732
- 620 Peter, V., Wong, K., Narne, V. K., Sharma, M., Purdy, S. C., and McMahon, C. (2014).
621 “Assessing spectral and temporal processing in children and adults using temporal
622 modulation transfer function (TMTF), iterated ripple noise (IRN) perception, and
623 spectral ripple discrimination (SRD),” *J. Am. Acad. Audiol.*, **25**, 210–218.
624 doi:10.3766/jaaa.25.2.9

- 625 Rom, D. M. (1990). "A sequentially rejective test procedure based on a modified Bonferroni
626 inequality," *Biometrika*, **77**, 663–666.
- 627 Saoji, A. A., Litvak, L., Spahr, A. J., and Eddins, D. A. (2009). "Spectral modulation
628 detection and vowel and consonant identifications in cochlear implant listeners," *J.*
629 *Acoust. Soc. Am.*, **126**, 955–8. doi:10.1121/1.3179670
- 630 Shannon, R., Zeng, F. G., Kamath, V., Wygonski, J., and Ekelid, M. (1995). "Speech
631 recognition with primarily temporal cues," *Science (80-.)*, **270**, 303–304.
- 632 Stone, M. A., Füllgrabe, C., and Moore, B. C. J. (2008). "Benefit of high-rate envelope cues
633 in vocoder processing: effect of number of channels and spectral region," *J. Acoust. Soc.*
634 *Am.*, **124**, 2272–82. doi:10.1121/1.2968678
- 635 Supin, A. Y., Popov, V. V, Milekhina, O. N., and Tarakanov, M. B. (1994). "Frequency
636 resolving power measured by rippled noise," *Hear. Res.*, **78**, 31–40. Retrieved from
637 <http://www.ncbi.nlm.nih.gov/pubmed/7961175>
- 638 Supin, A. Y., Popov, V. V, Milekhina, O. N., and Tarakanov, M. B. (1998). "Ripple density
639 resolution for various rippled-noise patterns," *J. Acoust. Soc. Am.*, **103**, 2042–2050.
640 doi:10.1121/1.421351
- 641 Wilcox, R. (2012). *Modern statistics for the social and behavioral sciences A practical*
642 *introduction*, CRC Press, New York, 1st ed., 1-22 pages.
- 643 Wilcox, R. (2012). *Introduction to robust estimation and hypothesis testing*, Academic Press,
644 Oxford, UK, Third Edit., 2-17 pages. doi:10.1016/B978-0-12-386983-8.00005-6
- 645 Won, J. H., Drennan, W. R., and Rubinstein, J. T. (2007). "Spectral-ripple resolution
646 correlates with speech reception in noise in cochlear implant users," *J. Assoc. Res.*
647 *Otolaryngol.*, **392**, 384–392. doi:10.1007/s10162-007-0085-8
- 648 Yost, W. A., Patterson, R. D., and Sheft, S. (1996). "A time domain description for the pitch
649 strength of iterated rippled noise," *J. Acoust. Soc. Am.*, **99**, 1066–1078.
- 650
- 651
- 652